Arch Appl Mech (2012) 82:879–890
DOI 10.1007/s00419-011-0598-9

ORIGINAL

Mehran Mirramezani · Hamid Reza Mirdamadi

The effects of Knudsen-dependent flow velocity on vibrations of a nano-pipe conveying fluid

Received: 26 October 2011 / Accepted: 2 December 2011 / Published online: 15 December 2011

Abstract In this paper, we investigate the effect of nano-flow on vibration of nano-pipe conveying fluid using Knudsen (Kn). We use Euler–Bernoulli plug-flow beam theory. We modify no-slip condition of nano-pipe conveying fluid based on Kn. We define a Kn-dependent flow velocity. We consider effect of slip condition, for a liquid and a gas flow. We reformulate Navier–Stokes equations, with modified versions of Kn-dependent flow velocity. We observe that for passage of gas through nano-pipe with nonzero Kn, the critical flow velocities decreased considerably as opposed to those for zero Kn. This can show that ignoring Kn effect on a gas nano-flow may cause non-conservative design of nano-devices. Furthermore, a more impressive phenomenon happens in the case of clamped-pinned pipe conveying gas fluid. While we do not observe any coupled-mode flutter for a zero Kn, we can see the coupled-mode flutter, accompanying the second-mode divergence, for a nonzero Kn.

Keywords Nano-scale effects · Knudsen-dependent flow velocity · Fluid-structure interaction (FSI) · Nano-flow · Slip boundary condition · Knudsen number (Kn)

1 Introduction

Carbon nano-tubes (CNTs), discovered by Iijima [1] in 1991, are effectively long, thin cylinders of graphite. The laboratory studies have shown that CNTs exhibit superior mechanical, thermal, optical, and electronic properties over any known material, so CNTs are currently being used or considered for a number of significant applications like: micro/nanoelectromechanical devices (MEMS/NEMS), hydrogen storage, micro/nano-actuators and artificial muscles. Due to perfect hollow cylindrical geometry and superior mechanical strength, CNTs have potential usage as gas storage devices or nano-vessels for conveying and storing fluids and drug delivery in bionanotechnology. In this regard, a remarkable number of studies have been accomplished to disclose the vibrational behavior of such nanostructures. However, in this paper, we are considering how the small-size effects of flow field influence the vibrational behavior of CNT. The Knudsen number (Kn), i.e., the dimensionless ratio of the mean free path of the fluid molecules to a characteristic length of the flow geometry, is used as a discriminant for identifying the different flow regimes. Based on Kn, four flow regimes may be identified: (1) $0 < \mathrm{Kn} < 10^{-2}$ for the continuum flow regime, (2) $10^{-2} < \mathrm{Kn} < 10^{-1}$ for the slip flow regime, (3) $10^{-1} < \mathrm{Kn} < 10$ for the transition flow regime, and (4) $\mathrm{Kn} > 10$ for the free molecular flow regime [2]. For

M. Mirramezani · H. R. Mirdamadi(✉)
Department of Mechanical Engineering,
Isfahan University of Technology,
84156-83111 Isfahan, Iran
E-mail: hrmirdamadi@cc.iut.ac.ir

M. Mirramezani
E-mail: mehranmirramezani@yahoo.com

CNTs conveying fluids, the Kn may be larger than 10^{-2}. Consequently, the assumption of no-slip boundary conditions is no longer valid, and a modified model shall be presented to reach more accurate results on the vibrational characteristics of CNTs conveying fluid. Several researchers studied about different kinds of stability for CNTs conveying fluid. For instance, Yoon et al. [3] studied the influence of internal flow on free vibration and flow-induced structural instability of CNT. They showed that the internal moving fluid could substantially affect vibrational frequencies especially for suspended, longer, and larger-innermost-radius CNTs at higher flow velocity and also revealed that a compliant surrounding elastic medium could significantly reduce the effect of internal moving fluid on resonant frequencies. Wang et al. [4] investigated the buckling instability of double-walled CNT conveying fluid by using a multi-elastic beam model and showed that the effect of the van der Waals force, the slenderness ratio and the spring constant of surrounding elastic medium on the critical flow velocity were significant. Chang and Lee [5] revealed that the effects of rotary inertia and transverse shear deformation reduced the vibration frequencies. Wang and Ni [6] found that during the flow of a fluid through a nano-tube, modeled as a continuum beam, the effect of viscosity of flowing fluid on the vibration and instability of CNTs could be ignored. Zhen and Fang [7] investigated the thermal and nonlocal effects on the vibration and instability of single-walled CNT conveying fluid and indicated that the natural frequencies and critical flow velocity increased as the temperature changes increased, and thermal effect could reduce the influence of nonlocal effect, whereas the nonlocal effect was enhanced as the flow velocity increased. These researchers used different methods to consider the small-size effects of CNTs conveying fluid, like numerical molecular dynamics (MD) simulations and nonlocal elasticity, but to the authors' knowledge, none of them considered an analytical approach to take into account for the small-size effects on the fluid flow side of this challenge. A key dimensionless parameter for discriminating fluid micro/nano-flows is Kn, which is the ratio of the fluid molecular mean free path to a characteristic length of the channel. For nano- and microchannels, the characteristic length is considered to be the radius of the channel. With due attention to that, in CNTs, Kn is considered to be higher than 10^{-2}. Thus, in such flow regimes, slip boundary conditions should be implemented, and the conventional Navier–Stokes equations are no longer valid. Hence, some modifications in the flow equations are necessary to obtain more accurate results for vibration of CNTs conveying fluid.

The numerical simulations of micro/nano-flows have been widely reported in the literature [8,9]. The theoretical foundations of these flow regimes are relatively well developed, such as slip boundary conditions [10,11], that is of our concern in this research. For slip flow regime, i.e., $0.01 < \mathrm{Kn} < 0.1$, the no-slip boundary condition theory fails, and a sublayer, namely, Knudsen layer, is a non-negligible part of the fluid flow from the wall surface. Thus, this phenomenon leads to a finite velocity slip, tangent to the wall surface. For Kn higher than 0.01, the slip velocity increases; thus, for slip flow regimes, Navier–Stokes continuum equations might be used with some care and modifications. At first, rarefaction effects should be taken into account [12]. Some methods have been presented for solving the nano-scale flow of fluids such as: (1) Direct simulation of monte carlo method (DSMC), (2) Lattice Boltzmann Method (LBM), (3) Molecular dynamics method (MD), and so on. All of these methods necessitate relatively large amounts of computational effort, cost, and time [2].

The main objective of this paper is to present an innovative model, for the coupled vibrations of nano-tube conveying fluid, considering the small-size effects in flow field. In our theory, we have presented a modified model that incorporates slip boundary conditions on the nano-tube walls. We have studied the effect of Kn on the critical velocities, velocities at which divergence and flutter instabilities may occur. Furthermore, we have utilized Galerkin weighted-residual method to solve the Fluid-structure interaction (FSI) governing partial differential equations and discretized our system by choosing more than two generalized coordinates, so we can show flutter instability in addition to divergence instabilities in the first and second modes of vibration.

The remainder of the paper is organized as follows: In Sect. 2, we present how to model the slip boundary conditions. In Sect. 3, we rederive the FSI governing equations by considering the slip boundary conditions. In Sect. 4, we implement the Galerkin weighted-residual solution technique and solve the partial differential equations of the nano-tube vibrations. In Sect. 5, we discuss stability analysis and present the results. Finally, in Sect. 6, we express our concluding remarks.

2 Modeling slip boundary conditions

We consider a flow field in a nano-channel with slip boundary conditions. The axial flow velocity with some higher-order slip boundary condition terms can be expressed as follows [2]:

$$V = V_0 + (\mathrm{Kn})^1 V_1 + (\mathrm{Kn})^2 V_2 + (\mathrm{Kn})^3 V_3 + O(\mathrm{Kn})^4 \tag{1}$$

where V is the axial flow velocity through the pipe. The technique of estimating $V_i, i = 0, 1, 2, \ldots$ are presented by Karniadakis et al. [2]. We are now in a position to reformulate the popular Navier–Stokes equations by substituting Eq. (1) into those equations for different orders of Kn.

Beskok and Karniadakis [13] suggested Eq. (2) as a slip velocity model, which is claimed to be rather a more representative relation for correlating with the experimental data:

$$V_s - V_w = \left(\frac{2-\sigma_v}{\sigma_v}\right)\left(\frac{\mathrm{Kn}}{1-b\mathrm{Kn}}\right)\left(\frac{\partial V}{\partial \mathrm{n}}\right) \tag{2}$$

where b is a general slip coefficient. By choosing $b = -1$, one can make the effect of slip condition as accurate as a second-order term. In Eq. (2), V_s is the slip velocity of the fluid near the CNT wall surface, V_w is the axial rigid body solid wall velocity, and n is the outward normalized unit normal vector to the CNT wall surface. σ_v is tangential momentum accommodation coefficient and is considered to be 0.7 for most practical purposes [14]. In this paper, we will utilize Navier–Stokes equations with Eq. (2) as a modeling tool for the slip velocity boundary condition.

3 Derivation of the fluid-structure interaction (FSI) governing equations

The governing equations for the conventional FSI problems have been derived by the assumption of no-slip boundary conditions. With due attention to the Kn for CNTs, this condition is no longer valid, so we have to use the conventional Navier–Stokes equations but satisfy the slip boundary conditions on the tube walls and find out an average velocity correction factor that relates the average velocity of no-slip and slip boundary conditions together.

Hence, consider a fully developed, incompressible, and viscous fluid flow of constant density and viscosity passing through a nano-tube. For a Newtonian fluid with a constant pressure gradient and neglecting the effect of gravitational body force, the well-known Navier–Stokes equations are stated as follows [15]:

$$\rho\frac{D\vec{V}}{Dt} = -\vec{\nabla}P + \mu\,\nabla^2\,\vec{V} \tag{3}$$

where ρ is the mass fluid density, P is the pressure, and D/Dt is the material derivative. In the above equation, we have to use the effective viscosity of a fluid in the slip regime by considering the small-size effects. Polard and Present [16] proposed the following equation for the effective viscosity of fluid as a function of Kn, which was suggested by Beskok and Karniadakis [13] as well:

$$\mu_e = \mu_0\left(\frac{1}{1+aKn}\right) \tag{4}$$

where μ_e is the effective viscosity, μ_0 is the bulk viscosity, and a is a coefficient and can vary from zero to a constant value, as follows [2]:

$$a = a_0\frac{2}{\pi}[\tan^{-1}(a_1 Kn^B)] \tag{5}$$

The values, $a_1 = 4$ and $B = 0.04$, are some empirical parameters. The coefficient a_0 can be obtained from free molecular regime and is formulated as [2]:

$$\lim_{Kn\to\infty} a = a_0 = \frac{64}{3\pi(1-\frac{4}{b})} \tag{6}$$

By these assumptions, the solution of Navier–Stokes equations in the axial direction of cylindrical orthogonal coordinates is as follows [15]:

$$V = \frac{1}{4\mu_e}\left(\frac{\partial P}{\partial x}\right)r^2 + C_3\ln(r) + C_4 \tag{7}$$

where r is the radius of the tube and x is longitudinal coordinate of tube elastic axis and axial flow. The boundary conditions enforce $C_3 = 0$. In order to obtain C_4, we use the slip boundary conditions at the CNT wall:

$$V_{(r=R)} = R\left(\frac{\sigma_v - 2}{\sigma_v}\right)\left(\frac{\mathrm{Kn}}{1 - b\mathrm{Kn}}\right)\left(\frac{\partial V}{\partial r}\right)_{r=R} \tag{8}$$

where R is the inner radius of the CNT Thus, Eq. (7) may be written as:

$$V_{\mathrm{slip}} = \frac{1}{4\mu_0\left(\frac{1}{1+aKn}\right)}\left(\frac{\partial P}{\partial x}\right)\left[r^2 - R^2 - 2R^2\left(\frac{2-\sigma_v}{\sigma_v}\right)\left(\frac{\mathrm{Kn}}{1+\mathrm{Kn}}\right)\right] \tag{9}$$

On the other hand, for no-slip boundary conditions, we choose $\mathrm{Kn} = 0$, and finally, Eq. (10) represents an average velocity correction factor:

$$\mathrm{VCF} \equiv \frac{V_{\mathrm{avg,slip}}}{V_{\mathrm{avg,(no-slip)}}} = (1 + a\mathrm{Kn})\left(1 + 4\left(\frac{2-\sigma_v}{\sigma_v}\right)\left(\frac{\mathrm{Kn}}{1+\mathrm{Kn}}\right)\right) \tag{10}$$

From now on, by considering the average velocity correction factor, we can use the popular FSI governing equations, and it is just adequate to replace the $V_{\mathrm{avg,slip}}$ by $\mathrm{VCF} \times V_{\mathrm{avg,(no-slip)}}$, in the fundamental equations. According to Paidoussis [17], we model the kinematics of the CNT nanostructure by Euler–Bernoulli plug-flow beam theory (EBPF). It should be noted that this model is adequate for pipes conveying fluid with a large aspect ratio of the length to the diameter, e.g., more than 10.

If we neglect the gravity, internal damping, externally imposed tension, pressurization, and elastic foundation effects, but consider only the effects of viscosity, the dimensionless equation of vibration of nano-tube conveying fluid is:

$$\frac{\partial^4\eta}{\partial\xi^4} + (u_{\mathrm{avg,slip}})^2\frac{\partial^2\eta}{\partial\xi^2} + 2\beta^{\frac{1}{2}}u_{\mathrm{avg,slip}}\frac{\partial^2\eta}{\partial\xi\partial\tau} + \frac{\partial^2\eta}{\partial\tau^2} - \psi_e\beta^{\frac{1}{2}}\frac{\partial^3\eta}{\partial\xi^2\partial\tau} - \psi_e u_{\mathrm{avg,slip}}\frac{\partial^3\eta}{\partial\xi^3} = 0 \tag{11}$$

where η is dimensionless lateral deflection; ξ, dimensionless axial coordinate; β, dimensionless mass parameter; u, dimensionless axial flow velocity; τ, dimensionless time parameter, and ψ is dimensionless viscosity parameter. In our case, the following dimensionless parameters have been arisen [17]:

$$(a)\tau = \left(\left[\frac{EI}{m_c + m_f}\right]\right)^{\frac{1}{2}}\frac{t}{L^2}, (b)\zeta = \frac{x}{L}, (c)\eta = \frac{W}{L}, (d)\beta = \frac{m_f}{m_c + m_f} \tag{12}$$

$$(a)u_{avg,(slip)} = \left(\frac{m_f}{EI}\right)^{\frac{1}{2}}L \times V_{avg,(slip)}, (b)\psi_e = \frac{\mu_e A_i}{(EIm_f)^{\frac{1}{2}}}, (c)\psi_0 = \frac{\mu_0 A_i}{(EIm_f)^{\frac{1}{2}}} \tag{13}$$

where E is the CNT Young's modulus modeled as an Euler–Bernoulli plug-flow beam theory; I, the area cross-sectional moment of inertia; m_f, the fluid mass per unit length. Other parameters are m_c, the CNT mass per unit length; t, time; L, the characteristic length of the nano-channel; w, the flexural displacement of the CNT wall in z-direction Cartesian coordinate system; and A_i, the cross-sectional area of the fluid passing through the CNT. By considering the average velocity correction factor and the effective bulk viscosity, the dimensionless equation of vibration upgrades to the following:

$$\begin{aligned}&\tfrac{\partial^4\eta}{\partial\xi^4} + (\mathrm{VCF})^2 \times (u_{\mathrm{avg,(no-slip)}})^2\tfrac{\partial^2\eta}{\partial\xi^2} + 2(\mathrm{VCF})\beta^{\frac{1}{2}} \times (u_{\mathrm{avg,(no-slip)}})\tfrac{\partial^2\eta}{\partial\xi\partial\tau} + \tfrac{\partial^2\eta}{\partial\tau^2}\\ &- \left(\tfrac{1}{1+aKn}\right)\psi_0\beta^{\frac{1}{2}}\tfrac{\partial^3\eta}{\partial\xi^2\partial\tau} - \left(\tfrac{1}{1+aKn}\right)\psi_0(\mathrm{VCF})(u_{\mathrm{avg,(no-slip)}})\tfrac{\partial^3\eta}{\partial\xi^3} = 0\end{aligned} \tag{14}$$

According to Wang and Ni [6], the effect of viscosity of flowing fluid on the vibration and instability of nanotubes may be ignored, so in our studies, we choose the bulk viscosity equal to zero and the final equation we use is:

$$\frac{\partial^4\eta}{\partial\xi^4} + (\mathrm{VCF})^2 \times (u_{\mathrm{avg,(no-slip)}})^2\frac{\partial^2\eta}{\partial\xi^2} + 2(\mathrm{VCF})\beta^{\frac{1}{2}} \times (u_{\mathrm{avg,(no-slip)}})\frac{\partial^2\eta}{\partial\xi\partial\tau} + \frac{\partial^2\eta}{\partial\tau^2} = 0 \tag{15}$$

To the authors' knowledge and experience, the above equation is capable of capturing the small-size effects on the fluid flow side of nano-scale FSI problems, i.e., by slip boundary condition effects in nano-flow regimes.

4 Galerkin weighted-residual solution technique

To solve the above equations and calculate the CNT complex-valued eigen-frequencies and present divergence and flutter instabilities, we use Galerkin approximate solution method. This is approximate, not only in a strict numerical sense, but also because of the finite number of terms utilized in the series solution expansion. Let:

$$\eta(\xi, \tau) \cong \sum_{n=1}^{N} \Phi_n(\xi) q_n(\tau) \tag{16}$$

where $q_n(\tau)$ are the generalized coordinates of the discretized system and $\Phi_n(\xi)$ are the dimensionless eigenfunctions of a beam with the same boundary conditions as the nano-pipe under consideration. It is presumed that the series may be truncated at a suitably high value of n. We use this method for two different boundary conditions, simply supported (pinned–pinned) and clamped-pinned ends. For a simply supported beam, the $\Phi_n(\xi)$ are derived as the following [18]:

$$\Phi_n(\xi) = \sin(k_n \xi), \quad n = 1, 2, \ldots, N, \tag{17}$$

where the wave numbers are as follows:

$$k_n = n\pi, \quad n = 1, 2, \ldots, N \tag{18}$$

The essential and natural boundary conditions for a simply supported beam are as follows:

$$\eta = 0 \quad \text{and} \quad \frac{\partial^2 \eta}{\partial \xi^2} = 0 \quad \text{at} \quad \xi = 0 \quad \text{and} \quad \xi = 1 \tag{19}$$

Both the essential and natural boundary conditions are satisfied by Eq. (17). By substituting Eq. (17) into (16), considering the weighted-orthogonality properties of eigen-mode shapes and integrating over the BVP domain, $\mathcal{D} = [0, 1]$, it leads to the vector ordinary differential equations for the vector $\{q_n(\tau)\}$, as follows:

$$[M]\{\ddot{q}_n(\tau)\} + [G]\{\dot{q}_n(\tau)\} + ([K_G] + [K_B])\{q_n(\tau)\} = 0 \tag{20}$$

The matrices $[M]$, $[G]$, $[K_B]$ and $[K_G]$ are the lumped-parameter nano-tube plus fluid dimensionless mass matrix, dimensionless gyroscopic matrix, dimensionless elastic internal bending stiffness matrix, and dimensionless geometric stiffness matrix, respectively. The gyroscopic matrix is due to Coriolis acceleration effects, and the geometric stiffness matrix is due to centripetal acceleration effects, both due to observing the fluid velocity as seen from a non-inertial reference frame attached to the vibrating nano-tube wall. The gyroscopic matrix is skew-symmetric, $[G] = -[G]^T$. All the other are symmetric matrices.

Calculating the above structural dynamics property matrices, the results are as the following:

The dimensionless mass matrix:

$$[M]_{ij} = [M]_{ji} = \frac{1}{2}\delta_{ij}, \quad i, j = 1, 2, \ldots, N. \tag{21}$$

where δ_{ij} is Kronecker delta.

The dimensionless gyroscopic matrix:

$$[G]_{ij} = -[G]_{ji} = 4\beta^{\frac{1}{2}} u \frac{ij}{i^2 - j^2}, \quad i \neq j, [G]_{ij} = 0, \quad i = j. \tag{22}$$

The dimensionless stiffness related matrices:

$$([K_G] + [K_B])_{ij} = \left(\frac{\pi^4 (ij)^2}{2}\right)\delta_{ij} - u^2 \left(\frac{(ij)\pi^2}{2}\right)\delta_{ij} \tag{23}$$

By substituting the above matrices into the system of ordinary differential equations (ODEs), we may assume the generalized coordinates $q_n(\tau)$, $n = 1, 2, \ldots, N$ vary as single harmonic motions (SHM) for a free vibration response:

$$q_n(\tau) = Z_n \exp(s_n \tau) \tag{24}$$

where s_n are complex-valued eigen-frequencies, whose real parts show the decaying rate in the nth modes (modal equivalent viscous damping), and the imaginary parts show the nth modal damped natural frequencies of the beam nanostructure, and Z_n are constant amplitudes of nth generalized coordinate of CNT free vibration. Furthermore, according to Eq. (13), the dimensionless eigen-frequencies Ω_n are related to the eigen-frequencies [17] (in terms of rad/s) as follow:

$$\Omega_n = \left(\frac{m_f + m_c}{\mathrm{EI}}\right)^{\frac{1}{2}} L^2 s_n \tag{25}$$

5 Results and discussions

In this section, we utilize the approximate solutions of Galerkin for simulating numerically the behavior of fluid passing through the nano-pipe. We consider the material and geometrical properties of nano-tube as, $\mathrm{E} = 1\,\mathrm{TPa}$, the thickness of CNT is $h = 10\,\mathrm{nm}$, $R_{\mathrm{out}} = 50$ nm, $\rho_{\mathrm{CNT}} = 2.3\,\mathrm{gr\,cm^{-3}}$, $L/2R_o = 500$. The fluid mass density is $\rho_{\mathrm{ace}} = 0.79\,\mathrm{gr\,cm^{-3}}$ for acetone, and $\rho_{\mathrm{air}} = 0.001169\,\mathrm{gr\,cm^{-3}}$ for air. In all numerical simulations, we have utilized three generalized coordinates and a constant aspect ratio. However, in the figures, we have shown only the first two eigen-frequencies.

5.1 Validation

In this subsection, we compare our numerical results with Paidoussis [17]. Figure 1 shows how the dimensionless imaginary parts of the first two eigen-frequencies of a pipe will change for the various values of dimensionless mean flow velocity of acetone through a simply supported pipe. In this case, the mean flow velocity is assumed based on classical Navier–Stokes continuum mechanics; i.e., Kn is zero. As we observe from Fig. 1, for a zero flow velocity, the dimensionless resonant frequencies of the pipe are π^2 and $(2\pi)^2$. These values for zero flow velocity are exactly the natural (undamped) frequencies of the pipe in free vibration. Their square values are proportional to the bending stiffness of the pipe. As the flow velocity increases from zero to a critical value, these frequencies approach zero, showing deterioration of the pipe bending stiffness. For critical flow velocities, the resonant frequencies become zero, and following them, the pipe stiffness disappears, and divergence or column buckling occurs. This is an important failure criterion for structural systems. From Fig. 1, we could see that the dimensionless critical flow velocity for the first mode divergence would be π and that of the second mode divergence, 2π, as we would expect from the observations of Paidoussis [17]. Figure 2 illustrates the same phenomenon for a clamped-pinned pipe. This time we have drawn the imaginary parts of eigen-frequencies in rad/s versus flow velocities in m/s. Again, in Fig. 2, Kn would be set to zero,

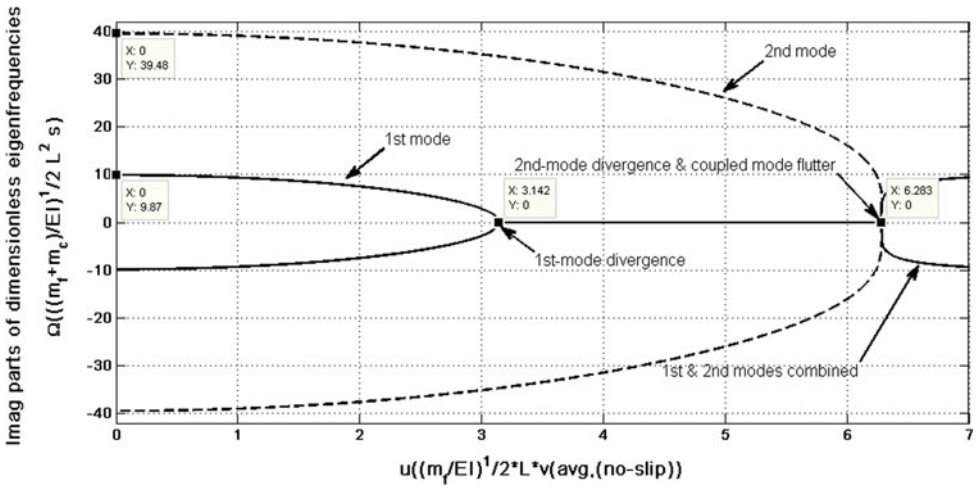

Fig. 1 Imaginary parts of dimensionless eigen-frequencies against dimensionless flow velocity for pinned–pinned nano-tube, for acetone, aspect ratio = 500, Kn = 0

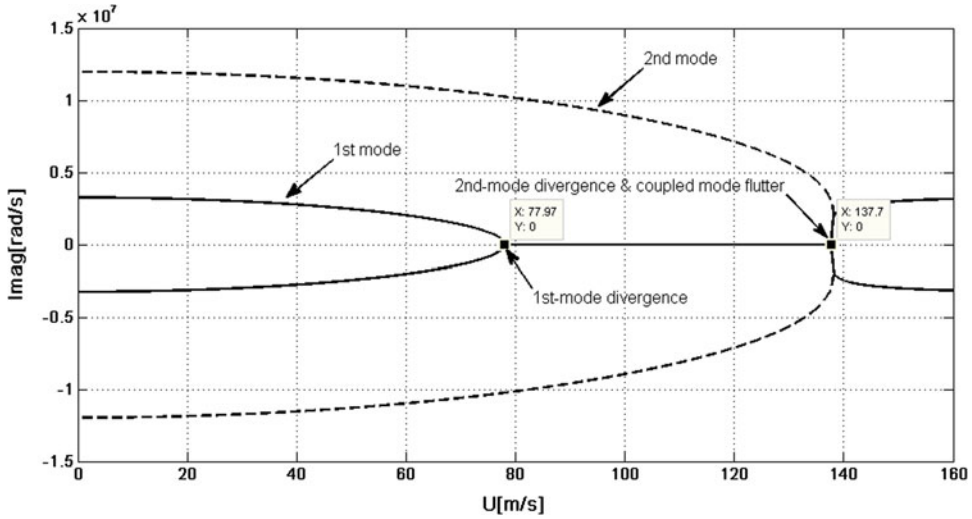

Fig. 2 Imaginary parts of eigen-frequencies of clamped-pinned nano-tube against flow velocity for acetone, aspect ratio = 500, Kn = 0

in order that we could have a validation with those references that either ignored the Kn effect or solved the problem for a macroscale flow. As may be seen from Fig. 2, the first critical flow velocity is equal to 77.97 m/s. Non-dimensionalizing it, we obtain dimensionless value of approximately 4.5634 that is in less than 2% error as compared with Paidoussis [17]. The second critical flow velocity is 137.7 m/s, with a dimensionless value of 8.0592, i.e., less than 4% error, compared with the same reference.

5.2 Liquid flow

In this subsection, we survey the effect of a nonzero Kn on the dynamic behavior of a nano-pipe conveying a liquid, herein, acetone. As indicated before, the range of Kn is from zero to 0.001. Figure 3a illustrates the imaginary parts of eigen-frequencies for a simply supported pipe conveying acetone and for two values of Kn equal to zero and 0.001. Due to little difference, we have drawn magnified parts of Fig. 3a, around the first and second mode divergence instability in Fig. 3b, and c, respectively. As it may be noticed, Kn has no appreciable effect on the general behavior of the coupled solid-fluid dynamics except that higher Kn may cause a positive shift in divergence happening, i.e., a higher Kn causes a sooner divergence. However, the difference is not so critical for a liquid nano-flow with a Kn at most equal to 0.001.

Figure 4a, shows the same information as Fig. 3a, for a pipe conveying fluid with clamped-pinned boundary conditions, and Fig. 4b and c are the zoomed-in graphs of Fig. 4a Again, we see that divergence and coupled mode flutter phenomenon happen in a lower critical flow velocity for a higher Kn. To the authors' knowledge, no one has reported this unmatured happening of pipe column buckling conveying a fluid. Still, someone may claim that the difference due to including the Kn effect is ignorable for a fluid nano-flow.

5.3 Gas flow

In this subsection, we discuss the same phenomenon for a nano-pipe conveying a gas fluid. Here, we have selected air with mass density 1.169 kg m^{-3}. Figures 5a through c illustrate and compare the evolutions of imaginary parts of the vibration eigen-frequencies of a simply supported nano-pipe against the flow velocity for three different Kn values of zero, one, and two. Figure 6a and b show the same information for a clamped-pinned pipe conveying a gas flow. Herein, the situations are totally different from those of liquid nano-flow. First, we observe from Fig. 5a through c that for higher Kn values than zero, critical flow velocities occur drastically sooner than that for the case of zero Kn.

This could be a great impact, for example, on the structural design of nano-sensors of fluidic device-type. The order of magnitude of the critical flow velocity has dropped approximately by more than one for the change in Kn from zero to two. A more interesting and striking phenomenon happens in the case of clamped-pinned

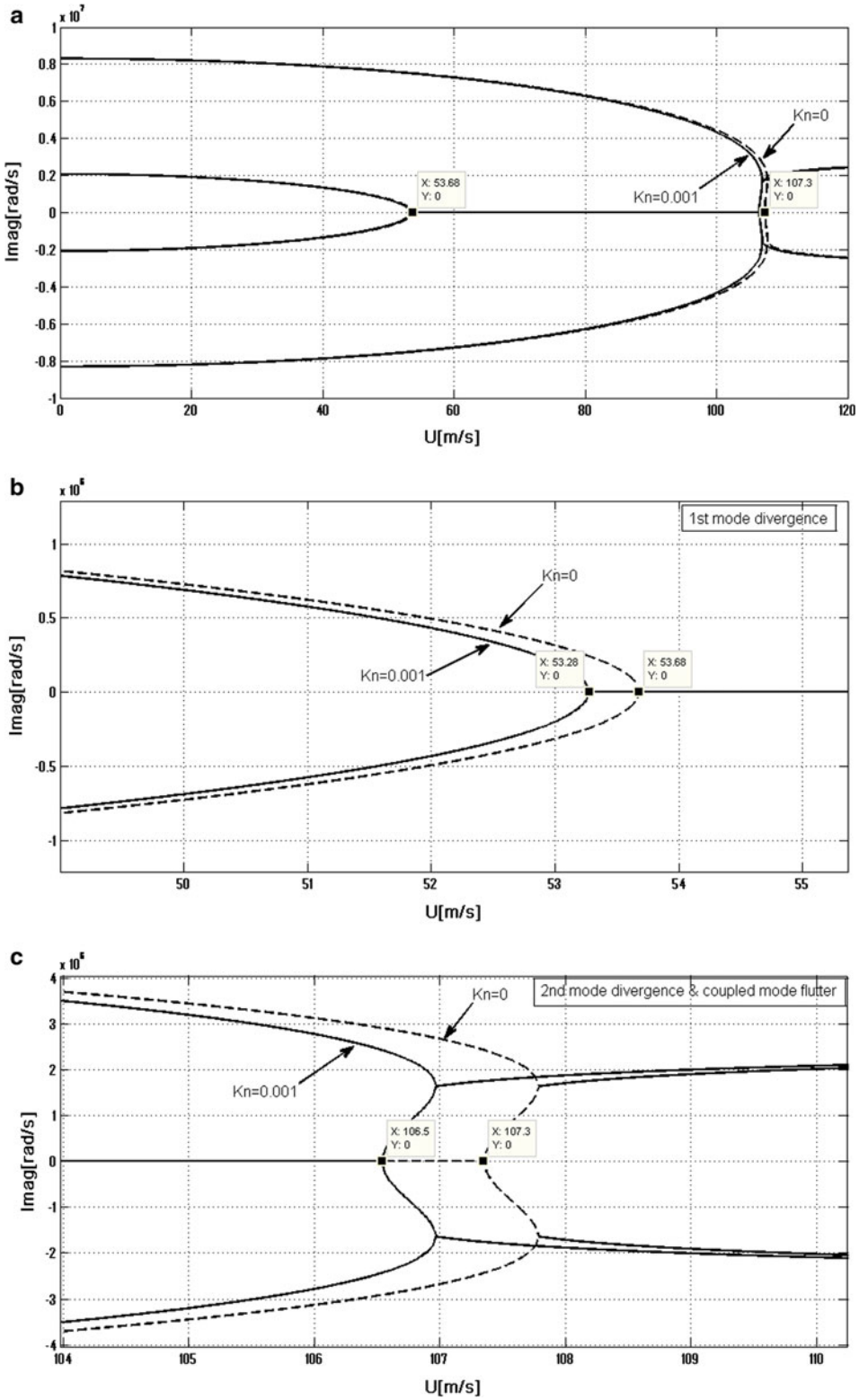

Fig. 3 **a** Imaginary parts of eigen-frequencies of pinned–pinned nano-tube against flow velocity for acetone, aspect ratio = 500, Kn = 0 and Kn = 0.001. **b** First mode divergence stability of pinned–pinned nano-tube, for acetone, aspect ratio = 500, Kn = 0 and Kn = 0.001 (zoom-in). **c** Second mode divergence and coupled mode flutter stabilities of pinned–pinned nano-tube, for acetone, aspect ratio = 500, Kn = 0 and Kn = 0.001, (zoom-in)

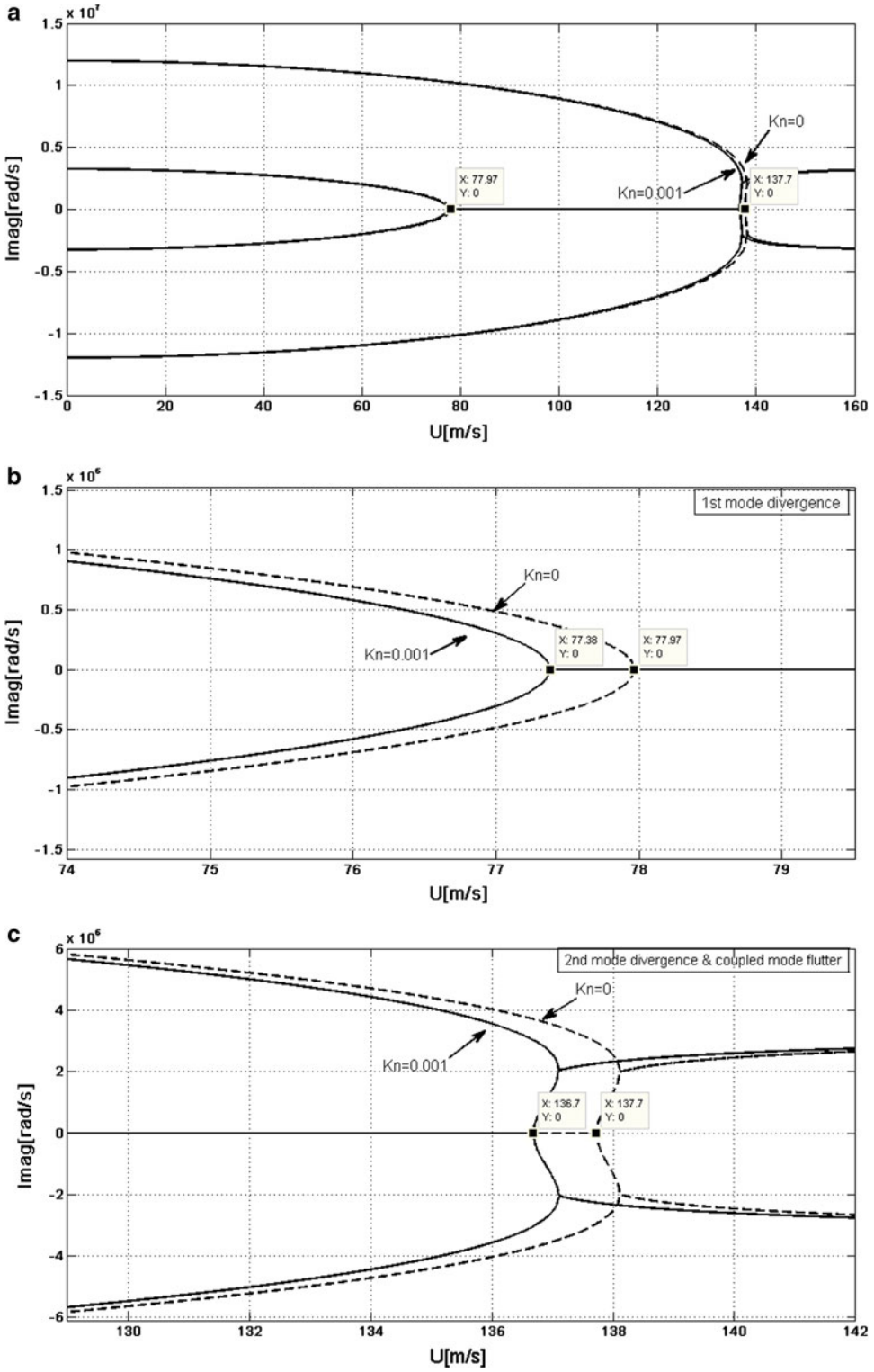

Fig. 4 **a** Imaginary parts of eigen-frequencies of clamped-pinned nano-tube against flow velocity for acetone, aspect ratio = 500, Kn = 0 and Kn = 0.001. **b** First mode divergence stability of clamped-pinned nano-tube, for acetone, aspect ratio = 500, Kn = 0 and Kn = 0.001 (zoom-in). **c** Second mode divergence and coupled mode flutter stabilities of clamped-pinned nano-tube, for acetone, aspect ratio = 500, Kn = 0 and Kn = 0.001, (zoom-in)

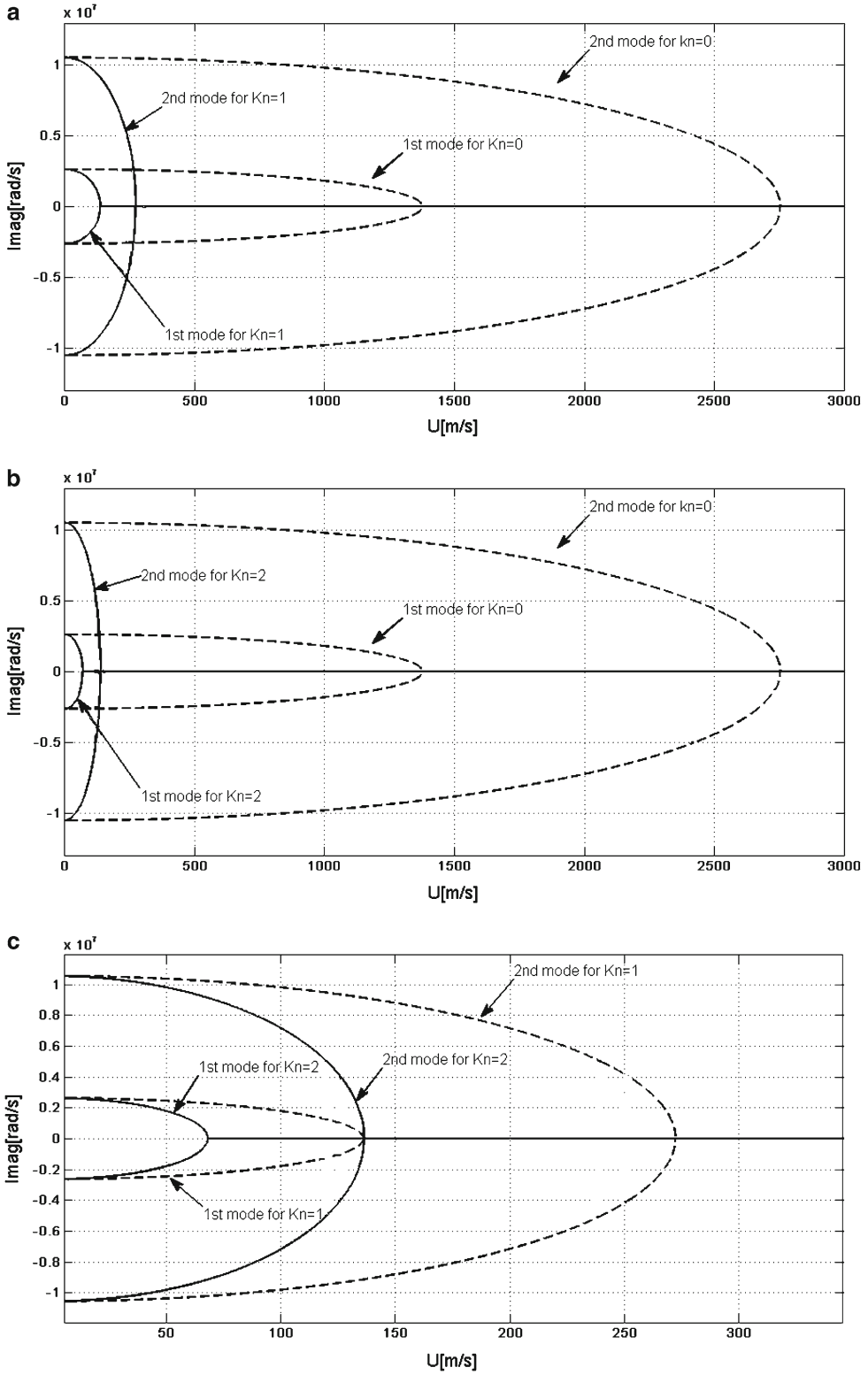

Fig. 5 **a** Imaginary parts of eigen-frequencies of pinned–pinned nano-tube against flow velocity for air, aspect ratio = 500, Kn = 0 and Kn = 1. **b** Imaginary parts of eigen-frequencies of pinned–pinned nano-tube against flow velocity for air, aspect ratio = 500, Kn = 0 and Kn = 2. **c** Imaginary parts of eigen-frequencies of pinned–pinned nano-tube against flow velocity for air, aspect ratio = 500, Kn = 1 and Kn = 2

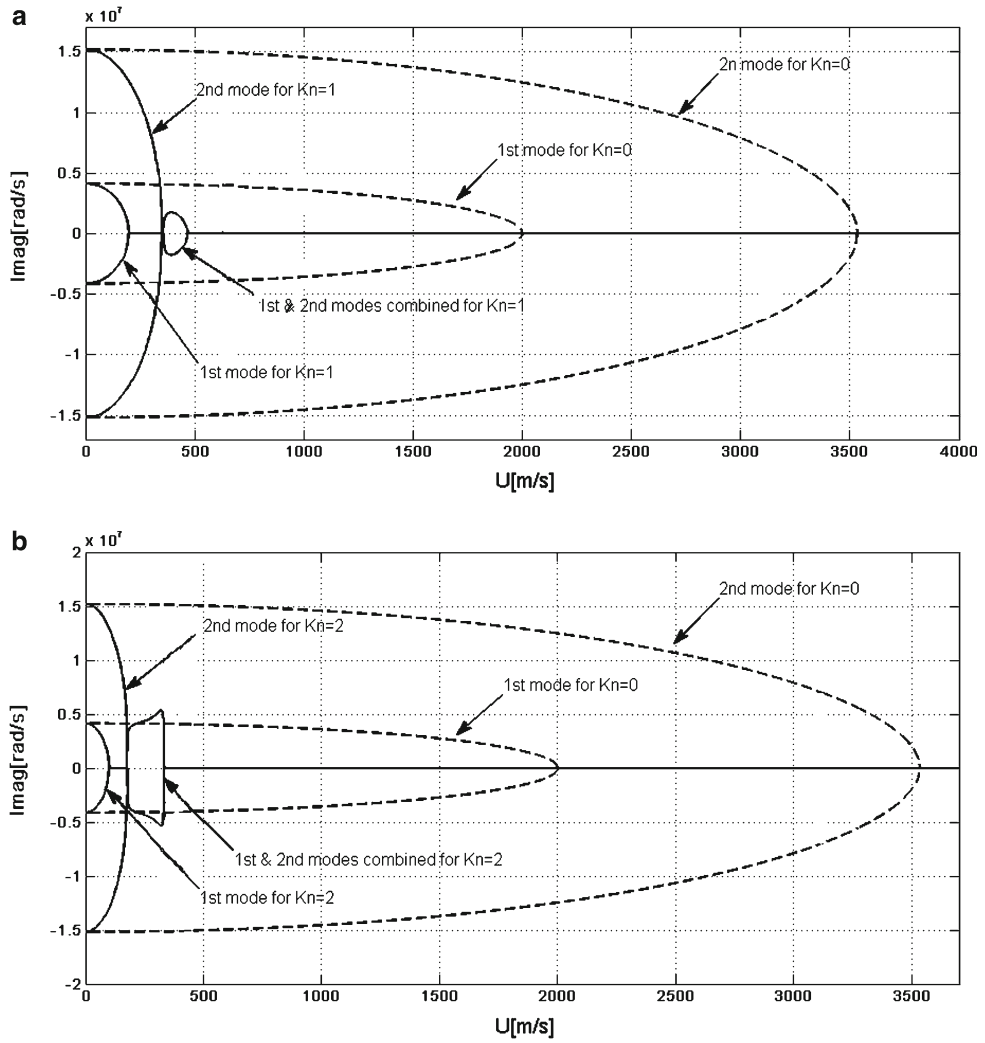

Fig. 6 **a** Imaginary parts of eigen-frequencies of clamped-pinned nano-tube against flow velocity for air, aspect ratio = 500, Kn = 0 and Kn = 1. **b** Imaginary parts of eigen-frequencies of clamped-pinned nano-tube against flow velocity for air, aspect ratio = 500, Kn = 0 and Kn = 2

pipe conveying gas fluid. While we do not observe any coupled-mode flutter for a Kn equal to zero, we can see the coupled mode flutter accompanying the second mode divergence for a Kn higher than zero. Still, the critical flow velocities for both modes of instability drop more intensively by increasing Kn from zero. We believe that this could be a shocking finding for the future of nano-technology.

6 Conclusions

In this research, we investigated the effect of a nano-size internal axial flow on the vibrational behavior of a nano-channel conveying fluid using Kn as a discriminant parameter for different flow regimes. We utilized the Euler–Bernoulli plug-flow (EBPF) kinematical theory for the interaction between the structural vibration and fluid motion. Although we modeled both the structure and the fluid by classical continuum mechanics constitutive laws, we modified the kinematic interface boundary condition between the vibration of solid wall and motion of fluid based on the value of Kn dimensionless parameter. Actually, we replaced the classical definition of flow velocity by a Kn-dependent flow velocity. We followed a similar procedure for redefining a Kn-dependent Newtonian viscosity law. For Kn equal to zero, we used normally the no-slip condition. We considered the effects of slip boundary condition, for both a liquid and a gas fluid flow. We reformulated a combination of Newton's second law of motion for an Euler–Bernoulli beam vibration and Navier–Stokes

equations for a fluid flow, with modified versions of Kn-dependent flow velocity and viscosity. We applied Galerkin method of weighted residuals to transform our BVP of fluid-structure interaction, including a PDE, geometric and natural boundary conditions, into a set of discretized ODEs. We simulated those ODEs with more than two generalized coordinates. However, we used only two of them for studying the results, for having higher accuracy. We analyzed the ODEs for a free vibration response and complex eigen-frequency calculations. We drew the imaginary parts of the first and second resonant frequencies against the flow velocity. We did this for different fluids (liquid and gas), Kn values, and structural boundary conditions. We observed that considering the no-slip boundary condition was not an influential parameter on the liquid nano-flow behavior with respect to a continuum flow regime. Considering the no-slip boundary condition could not change the critical liquid nano-flow velocity noticeably. However, the effect of slip condition over the nano-pipe wall was surprisingly striking for a gas nano-flow behavior. This is because of different Kn ranges for liquids and gases. For our selected materials and geometry, this range for liquids is approximately between 0.0 and 0.001 and for gases between 0.0 and 2.0. We observed that for the passage of a gas, like air, through the nano-pipe with any boundary condition and a Kn much higher than zero, e.g., 2, the critical velocities of the first and second mode divergence decreased considerably as opposed to those for Kn equal to zero. The order of magnitude of this reduction was more than one. This could show that ignoring Kn effect on a gas nano-flow might cause erroneously a non-conservative structural design of fluidic nano-devices. Yet, the critical gas flow velocities for both modes of divergence instability reduced more drastically than those of liquid flow, by increasing Kn from zero to two. Furthermore, A more interesting and impressive phenomenon happened in the case of clamped-pinned pipe conveying gas fluid. While we would not observe any coupled-mode flutter for a Kn equal to zero, we could see the coupled-mode flutter and mode combination, accompanying the second-mode divergence, for a Kn higher than zero, for gas flow.

References

1. Iijima, S.: Helical microtubules of graphitic carbon. Nature **354**, 56–58 (1991)
2. Karniadakis, G., Beskok, A., Aluru, N.: Microflows and Nanoflows: Fundamentals and Simulation. Springer, NY (2005)
3. Yoon, J., Ru, C.Q., Mioduchowski, A.: Vibration and instability of carbon nano-tubes conveying fluid. Compos. Sci. Technol. **65**, 1326–1336 (2005)
4. Wang, L., Ni, Q., Li, M.: Buckling instability of double-wall carbon nano-tubes conveying fluid. Comp. Mater. Sci. **44**, 821–825 (2008)
5. Chang, W.J., Lee, H.L.: Free vibration of a single-walled carbon nano-tube containing a fluid flow using the Timoshenko beam model. Phys. Lett. A **373**, 982–985 (2009)
6. Wang, L., Ni, Q.: A reappraisal of the computational modeling of carbon nano-tubes conveying viscous fluid. Mech. Res. Commun. **36**, 833–837 (2009)
7. Zhen, Y., Fang, B.: Thermal-mechanical and nonlocal elastic vibration of single-walled carbon nano-tubes conveying fluid. Comp. Mater. Sci. **49**, 276–282 (2010)
8. Hannon, L., Lie, G.C., Clementi, E.: Molecular dynamics simulation of channel flow. Phys. Lett. A **119**, 174–177 (1986)
9. Sun, M., Ebner, C.: Molecular-dynamics simulation of compressible fluid flow in two-dimensional channels. Phys. Rev. A **46**, 4813–4819 (1992)
10. Thompson, P.A., Troia, S.M.: A general boundary condition for liquid flow at solid surfaces. Nature **389**, 360–362 (1997)
11. Ellisab, J.S., Thompson, M.: Slip and coupling phenomena at the liquid-solid interface. Phys. Chem. **6**, 4928–4938 (2004)
12. Miguel, A.F., Serrenho, A.: On the experimental evaluation of permeability in porous media using a gas flow method. J. Phys. D Appl. Phys. **40**, 6824–6828 (2007)
13. Beskok, A., Karniadakis, G.E.: A model for flows in channels, pipes, and ducts at micro and nano scales. Microscale Thermophys. Eng. **3**, 43–77 (1999)
14. Shokouhmand, H., Isfahani, A.H.M., Shirani, E.: Friction and heat transfer coefficient in micro and nano channels filled with porous media for wide range of Knudsen number. Int. Commun. Heat Mass **37**, 890–894 (2010)
15. Shames, I.H.: Mechanics of Fluids. McGraw-Hill, NY (1982)
16. Polard, W.G., Present, R.D.: On gaseous self-diffusion in long capillary tubes. Phys. Rev. **73**, 762–774 (1948)
17. Paidoussis, M.D.: Fluid-Structure Interactions: Slender Structures and Axial Flow, vol. 1. Academic Press, London (1998)
18. Weaver, W., Timoshenko, S.P., Young, D.H.: Vibration Problems in Engineering. Wiley, NY (1990)